analytical chemistry

Article

pubs.acs.org/ac

Online Sample Conditioning for Portable Breath Analyzers

Amlendu Prabhakar,[†] Rodrigo A. Iglesias,[†] Xiaonan Shan,[†] Xiaojun Xian,[†] Lihua Zhang,[†] Francis Tsow,[†] Erica S. Forzani,[†,‡] and Nongjian Tao*[,†,§]

[†]Center for Bioelectronics & Biosensors, Biodesign Institute, [‡]School for Engineering of Matter, Transport and Energy, and [§]School of Electrical, Computer and Energy Engineering, Arizona State University, Tempe, Arizona 85287, United States

ABSTRACT: Various innovative chemical sensors have been developed in recent years to sense dangerous substances in air and trace biomarkers in breath. However, in order to solve real world problems, the sensors must be equipped with efficient sample conditioning that can, e.g., control the humidity, which is discussed much less in the literature. To meet the demand, a miniaturized mouthpiece was developed for personal breath analyzers. A key function of the mouthpiece is to condition the humidity in real breath samples without changing the analyte concentrations and introducing substantial backpressure, which is achieved with optimized packing of desiccant particles. Numerical simulations were carried out to determine the performance of the mouthpiece in terms of various controllable parameters, such as the size, density, and geometry of the packing. Mouthpieces with different configurations were built and tested, and the experimental data validated the simulation findings. A mouthpiece with optimized performance reducing relative humidity from 95% (27 000 ppmV) to 29% (8000 ppmV) whereas retaining 92% nitric oxide (50 ppbV to 46 ppbV) was built and integrated into a hand-held exhaled nitric oxide sensor, and the performance of exhaled nitric oxide measurement was in good agreement with the gold standard chemiluminescence technique. Acetone, carbon dioxide, oxygen, and ammonia samples were also measured after passing through the desiccant mouthpiece using commercial sensors to examine wide applicability of this breath conditioning approach.

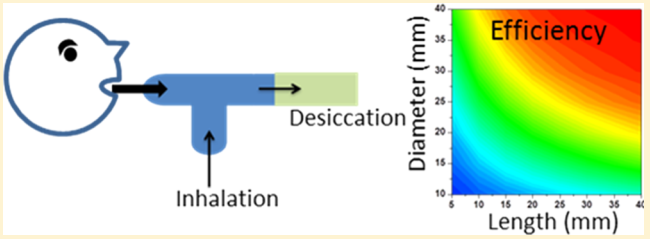

While most works on chemical sensors published to date are devoted to detection, sample collection and conditioning that often determine whether a sensor can solve a real world problem or not are much less emphasized. This is especially the case for breath analyzers. Human breath contains a variety of chemical signatures that are attractive for early detection and noninvasive management of diseases.[1,2] Some of these chemicals, such as nitric oxide, hydrogen, and ^{13}C urea, have already been used in clinical settings,[3−7] and many others have been studied and identified as potential biomarkers for different diseases and health conditions.[8,9] A difficult challenge in developing breath analyzers is to accurately measure a trace amount of analytes in the presence of not only hundreds of interfering gases but also highly concentrated water vapor. Human breath is nearly saturated with water vapor (>95% relative humidity, RH)[10,11] which coming out at body temperature condenses in the sensor and often leads to the failure of the breath analyzer, which requires proper sample conditioning before detection.[12,13]

A common solution to condition a high humidity sample is to introduce nafion tubing in the sampling line to reduce humidity. However, the reported efficiency of humidity reduction by nafion tubing is highly variable, ranging from 58% to 98% depending on ambient humidity.[14,15] For this reason, many applications must flow additional drying gas into the nafion tubing in order to maintain the efficiency,[16] which adds complexity into the device and also makes it unsuitable for personal use that requires portability. A more serious issue with the nafion approach is that it not only removes unwanted humidity but also partially or completely (75% to >90%) removes many wanted analytes, such as low-molecular-weight, polar, oxygenated compounds, including some ketones, alcohols, aldehydes, and water-soluble ethers.[14] These analytes are of high clinical significance for different diseases. Real time breath sample measurement without removal of humidity has been done using mass spectrometric platforms including selected ion flow tube (SIFT)[17,18] and proton transfer reaction (PTR)[19−21] mass spectrometry. These techniques employ special handling of breath sample to avoid humidity condensation and require long heated tubes and capillaries heated up to 100 °C.[22−24] In addition to conditioning the humidity of a breath sample, another critical requirement for a breath analyzer is to provide an appropriate volumetric flow rate and back pressure. The flow rate and back pressure requirements differ depending on specific guidelines for the analyte being measured. For example, in the case of breath nitric oxide, a biomarker for inflammation, the American Thoracic Society recommends that the back pressure should be at least 5 cm H_2O.[25]

As an effort to overcome the difficulties discussed above, we introduce here a breath sample conditioning approach based on desiccant particles packed in tubing, which can be integrated

Received: June 5, 2012
Accepted: July 18, 2012
Published: July 18, 2012

   dx.doi.org/10.1021/ac301542j | *Anal. Chem.* 2012, 84, 7172−7178

into the inlet of existing breath monitoring devices. We further establish the relationships of the output humidity, flow rate, and pressure in terms of controllable parameters, such as particle size and tubing geometry. The relationships are established based on numerical simulation and validated experimentally. Using this approach, we have designed mouthpieces for nitric oxide detection using a hand-held device.[26]

EXPERIMENTAL AND SIMULATION METHODS

Simulation Methods. Numerical simulation of the desiccation process in the mouthpiece was performed using finite element method software COMSOL multiphysics 3.5. The simulation included models for flow and mass transport in the porous medium of calcium chloride, which was used as a desiccant material to adsorb water and control humidity. Temperature change during the desiccation process was not taken into account for simplifying the model. It was experimentally observed that the temperature increased by about 20 °C at the mouthpiece inlet for 1 L of breath sample whereas the outlet temperatures increased by 1−2 °C. This rise in temperate did not have considerable effect on the working efficiency of the overall desiccant tube (Table 2) since enough material in the tube was far away from saturation. A 2-dimensional rectangular geometry with rotational symmetry, as shown in Figure 1, was used to simulate the cylindrical tubing.

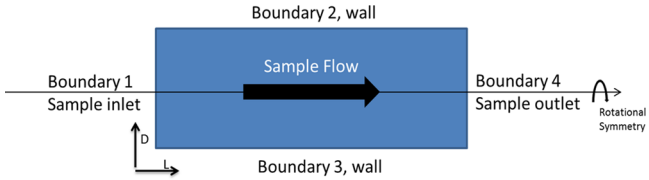

Figure 1. Representation of the modeling domain representing the cylindrical desiccation tube in two dimensions assuming a rotational symmetry of packing.

The tubing, defined as a subdomain, was packed with the desiccant particles of different diameters (d) into a porous structure, with porosity, ε_p, varying from 0.25 to 0.65. The permeability (κ) of the system for a given porosity and particle size was estimated by Kozeny's relation[27]

$$\kappa = \text{constant} \times \frac{d^2 \varepsilon_p^{\,3}}{(1-\varepsilon_p)^2} \tag{1}$$

The constant in the equation was determined experimentally to be 984 by measuring the sample flow rate (v) and pressure difference across a known length (Δx) of the mouthpiece using Darcy's law[28]

$$v = \frac{\kappa}{\eta}\frac{\Delta P}{\Delta x} \tag{2}$$

where η is the dynamic viscosity (1.74×10^{-5} Pa·s) of humid air at physiological temperature.[29]

Brinkman equations given by

$$\frac{\rho}{\varepsilon_p}\frac{\partial \mathbf{u}}{\partial t} + \nabla\cdot\left[-\frac{\eta}{\varepsilon_p}(\nabla\mathbf{u} + (\nabla\mathbf{u})^{\mathrm{T}}) + p\mathbf{I}\right] = -\frac{\eta}{\kappa}\mathbf{u} \tag{3}$$

$$\nabla\cdot\mathbf{u} = 0 \tag{4}$$

were used to model the flow of breath through this medium, where ρ denotes the density of humid air ($1.15\ \mathrm{kg\cdot m^{-3}}$), $\mathbf{u}$ represents the velocity, and p refers to the pressure. Equation 4 above implies that the fluid flow is incompressible in the subdomain. Since Mach number for the flow at $6.67\ \mathrm{L\cdot min^{-1}}$ through a typical mouthpiece geometry is less than 0.3, the only appreciable fluid density change resulted from change in temperature of the breath due to rise in desiccant temperature. The increase in breath temperature was measured to be less than 3 °C resulting in ∼1% increase in density for which the assumption of incompressible flow is valid. Boundary conditions for the flow were set as follows: Boundary 1: $\mathbf{u}\cdot\mathbf{n}$ = u0 (inlet), where u0 is the linear flow velocity at the inlet; Boundary 2 and Boundary 3: $\mathbf{u} = 0$ (wall); Boundary 4: $p = 0$ (outlet). With these subdomain and boundary settings, the velocity field was determined and the solution obtained was further used to solve the mass transport process using COMSOL 3.5.

Mass transport of water within the desiccant tube was described by the diffusion−convection equations

$$\frac{\partial C_i}{\partial t} + \nabla\cdot(D_i\nabla C_i + C_i\mathbf{u}_i) = R \tag{5}$$

where C_i denotes the concentration of the species, D is the diffusion coefficient, $\mathbf{u}$ represents the velocity, and R refers to the rate of consumption of species i. These equations were applied to the two components of the desiccation process, viz., humidity in the breath ($i = 1$) and the surface binding sites available on desiccant calcium chloride for capture of humidity ($i = 2$). For breath, the diffusion coefficient of water vapor was set to be $4.6 \times 10^{-7}\ \mathrm{m^2\cdot s^{-1}}$.[30] The boundary conditions were set as follows: Boundary 1: $C_1 = C_1^{\mathrm{in}}(1 - e^{-t/2})$ (inlet, allows humidity to rise from 0 to within 1% of the maximum breath humidity C_1^{in} in 10 s compensating for time lag due to sampling of nonalveolar dead space air); Boundary 2 and Boundary 3: $\mathbf{n}\cdot(D\nabla C_1 + C_1\mathbf{u}) = 0$ (wall); Boundary 4: $\mathbf{n}\cdot(D\nabla C_1) = 0$ (outlet, no convective flux).

For binding sites on the solid calcium chloride, diffusion was neglected and all the boundaries were set as wall for mass transfer [i.e., $\mathbf{n}\cdot(D\nabla C_2 + C_2\mathbf{u}) = 0$] assuming no inflow or outflow of the desiccant material through any boundary. The rate of water vapor consumption was given by the linear driving force approximation[31−33]

$$R = k_0(C^* - C^{\mathrm{s}}) \tag{6}$$

where k_0 is the mass transfer coefficient, obtained from parameter fitting to be $5.5 \times 10^{-3}\ \mathrm{s^{-1}}$, C^{s} represents the surface concentration of water on the calcium chloride surface at any given time, and C^* is its equilibrium value. Equilibrium water concentration was modeled through the Dubinin−Astakhov equation approximated as[34−36]

$$C^* = \frac{C_2^0 k_1 C_1}{1 + k_2 C_1} \tag{7}$$

where C_2^0 represented the initial concentration of binding sites on calcium chloride available for humidity capture and k_1 and k_2 were equilibrium parameters obtained from fitting, which were $0.33\ \mathrm{m^3\cdot mole^{-1}}$ and $0.01\ \mathrm{m^3\cdot mole^{-1}}$, respectively. The surface humidity concentration at any time was represented as

$$C^{\mathrm{s}} = C_2^0 - C_2 \tag{8}$$

Finally, the rate of consumption was obtained as

dx.doi.org/10.1021/ac301542j | Anal. Chem. 2012, 84, 7172−7178

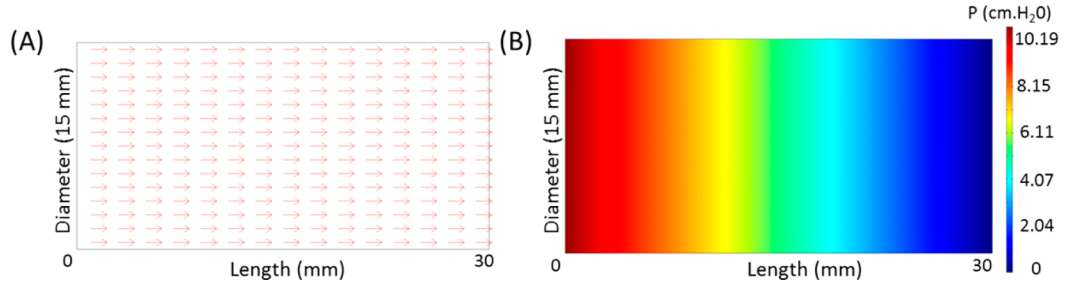

Figure 2. (A) Simulated velocity field along the tube shows uniform flow field established at a given flow rate of 6.67 L·min^{-1}, particle size of 1.15 mm, and porosity of 0.425. (B) Simulated pressure profile along the tube showing increasing back pressure with tube length assuming uniform packing density.

$$R = k_0\left[\frac{C_2^0 * k_1 C_1}{1 + k_2 C_1} - (C_2^0 - C_2)\right] \quad (9)$$

These mass balance equations with the appropriate boundary conditions described above were solved using COMSOL 3.5 coupled with the velocity field obtained earlier with the flow simulation to generate a concentration profile of breath humidity introduced into the desiccation tube.

Experimental Validation of Mouthpiece Performance. In order to experimentally validate the simulation results, several mouthpieces were prepared by packing desiccant particles into cylindrical tubes. Different particle sizes of the desiccant were obtained by refining anhydrous calcium chloride pellets (Fisher Scientific, 4−20 mesh). These refined particles were size selected by sieving through wire meshes of predefined sizes. Average particle sizes of 1.15 mm and 0.65 mm were chosen for use. A cylindrical plastic mouthpiece (VacuMed, Part# 1018-22) with internal diameter of 22 mm was used for packing these particles at porosity values of 0.425 and 0.365, respectively. Mouthpieces with three different lengths (12, 24, and 46 mm) were tested.

Humidity levels of the breath sample before and after passing through the mouthpiece were measured using a selected ion flow tube mass spectrometer (SIFT-MS) (Instrument science Ltd.) operating in multiple ion monitoring mode with H_3O^+ as the precursor ion.[17] The backpressure generated by the mouthpiece was measured using a pressure sensor (Freescale, Part# MP3 V5004G) at a fixed sample flow rate. Sample flow rate from pressurized gas container (Praxair, Breathing grade air) was controlled with pressure regulators and monitored with a mass flow meter (Sensirion, EM1).

Integration of the Mouthpiece with Breath Analyzers. The mouthpiece and a non-rebreathing T-valves (VacuMed, Part# 1464) were integrated into a portable breath nitric oxide sensor developed in our lab. The breath sensor was based on selective colorimetric change due to redox chemistry of phenylenediamine derivatives with the analyte.[26] Subjects blew directly into the mouthpiece for online measurement. The readings from the portable nitric oxide sensor were compared and correlated with chemiluminescence detection (Sievers NOA), which is the gold standard for nitric oxide measurement. Selective capture of humidity over some other gases by the desiccant material was tested with samples collected offline in metal laminated Tedlar bags at a flow rate of 6.7 L·min^{-1} using commercial sensors. Acetone and ammonia were measured with SIFT-MS; carbon dioxide was measured using an absorption infrared based hand-held monitor (Telaire 7000 Series), and oxygen was measured using a portable electrochemical sensor (Vascular technologies).

RESULTS AND DISCUSSIONS

Simulation. Flow and mass transfer simulations were carried for several mouthpiece configurations. Figure 2A

Table 1. Simulated Values of Back Pressure in cm H_2O Generated in the Desiccant Mouthpiece for Varying Porosities and Particle Sizes[a]

	porosity				
particle size (mm)	0.25	0.35	0.45	0.55	0.65
0.35	243.50	66.68	22.46	8.23	3.01
0.70	60.91	16.67	5.61	2.05	0.75
1.05	27.07	7.41	2.49	0.91	0.33
1.40	15.22	4.17	1.40	0.52	0.18

[a]Simulation is for 5 grams of calcium chloride.

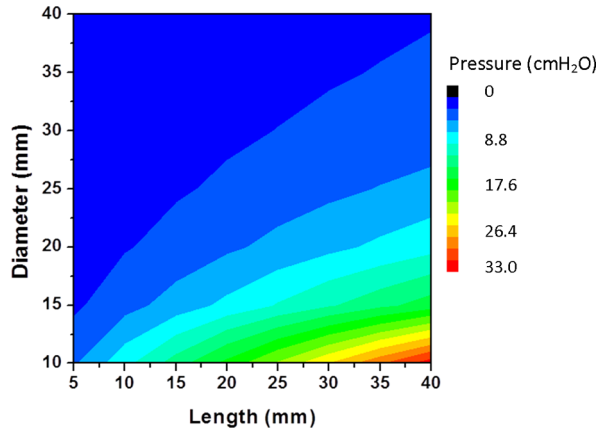

Figure 3. Pressure drop as a function of tube geometry for a given volumetric flow rate (6.67 L/min).

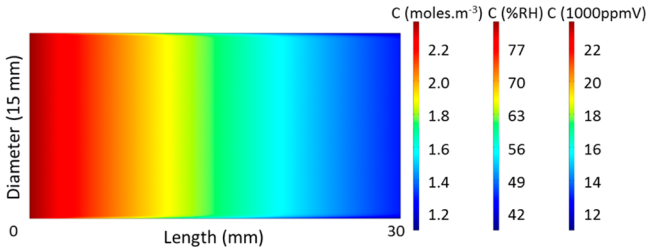

Figure 4. Simulation result of breath humidity concentration along the desiccation tube. Result is for a volumetric flow rate of 6.67 L/min and sampling time of 30 s through a desiccant tube (15 mm diameter, 30 mm length, 5 g of calcium chloride, 1.15 mm particle diameter, porosity of 0.425).

dx.doi.org/10.1021/ac301542j | Anal. Chem. 2012, 84, 7172−7178

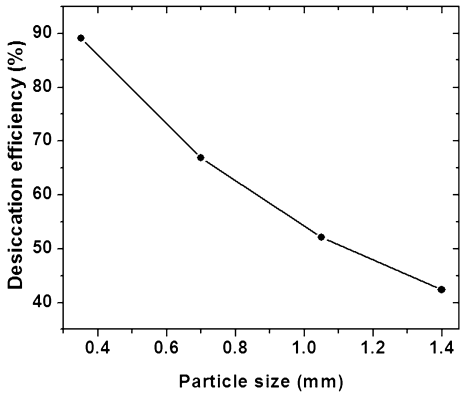

Figure 5. Desiccation efficiency for different particle sizes at a fixed geometry of the mouthpiece (15 mm long, 22 mm diameter) using 5 g of calcium chloride.

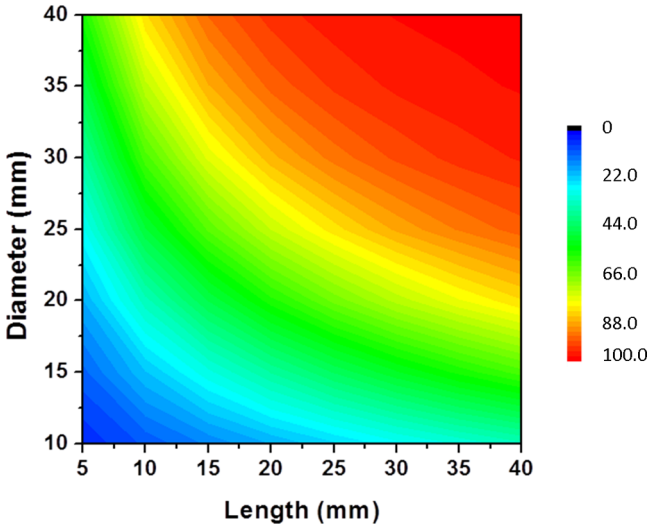

Figure 6. Desiccation efficiency simulated as a function of tube geometry for a given volumetric flow rate (6.7 L/min).

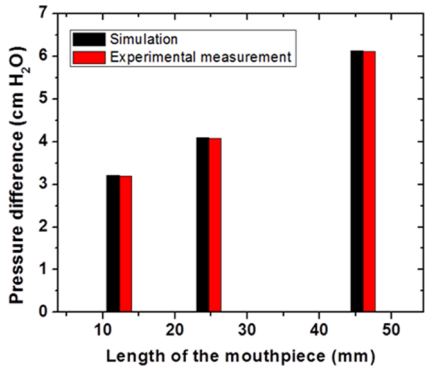

Figure 7. Comparison of simulated and experimentally measured pressure difference across the mouthpiece packed with 1.15 mm particles with a porosity of 0.425.

shows the flow profile obtained from a 30 mm long desiccant tube, 15 mm in diameter, packed with calcium chloride particles of 1.15 mm average diameter with a porosity of 0.425. For this porosity and particle size at a flow rate of 6.67 L·min^{-1}, the velocity field is homogeneous due to porous properties of the structure, which is in contrast to parabolic velocity fields generally obtained under similar conditions in a nonporous free channel. Figure 2B shows the simulated pressure profile along the tube. The pressure drop increases with the increasing length of the packing material at a given packing density. Values for back pressure resulting from different particle sizes and porosities of packing for a given amount (5 g) of calcium chloride were also calculated as shown in Table 1.

The data from Table 1 provides guidelines on packing of the desiccant material to achieve the desired back pressure range by changing either or both the particle size and the porosity of the mouthpiece. It is evident that back pressure at a given flow rate can be reduced by increasing either the particle size or the porosity of packing for a given mass of desiccant and mouthpiece geometry. Simulations were also carried out to obtain the effect of mouthpiece geometry (diameter and length) for a fixed particle size and porosity of packing assuming uniform packing density. Figure 3 plots pressure drop as a function of tube geometry with particles 1.15 mm in diameter packed with a porosity of 0.425. It is evident from the plot that the pressure drop decreases with increasing diameter and decreasing length of the mouthpiece for a given volumetric sample flow rate.

While providing an appropriate backpressure with the mouthpiece is an important requirement for many breath analyzers, other important parameters include the desiccation efficiency, which should be considered together with the backpressure. For this reason, the desiccation process was simulated. The desiccation of the breath along the tube (15 mm diameter, 30 mm length, 5 g of calcium chloride, 1.15 mm particle diameter, porosity of 0.425) is shown in Figure 4. Humidity of the sample decreases along the tube resulting in dryer output of the sample. Humidity levels at boundary 1 (inlet) and boundary 4 (outlet) were integrated for 30 s in order to calculate of the efficiency (output/input %) of the desiccation process.

Desiccation efficiencies with different particle sizes of the desiccant particles were simulated for a given flow and amount of desiccant. Figure 5 shows the desiccation efficiency decreasing with increasing particle size for 5 g of calcium chloride. The efficiency was found to be independent of the packing porosity under these conditions. Desiccation efficiencies were also simulated for a fixed particle size and packing porosity with changing mouthpiece geometry (length and diameter). Figure 6 shows a plot of desiccation efficiency as a function of mouthpiece geometry with 1.15 mm wide particles packed with a porosity of 0.425. It can be seen from the plot that the efficiency of desiccation improves with increasing length and diameter (i.e., volume) of the mouthpiece.

These simulation results are useful in choosing the best parameters for preparing a customized mouthpiece for any breath analyzers. These parameters include mouthpiece geometry (length and diameter), particle size, and packing porosity. It is also clear that if any of these parameters are constrained based on particular needs of a certain device then other parameters can be varied to achieve the desired performance.

Experimental Validation of Mouthpiece Performance.

In order to validate the flow simulation, mouthpieces with three different lengths and 22 mm diameter were prepared. This geometry was chosen for easy integration with our device. Figure 7 shows the comparison of simulated to measured pressure difference across the tube for the three chosen lengths. Both results correlate well showing that the pressure drop increases with increasing length of the mouthpiece.

dx.doi.org/10.1021/ac301542j | *Anal. Chem.* 2012, 84, 7172−7178

Table 2. Comparison of Simulated and Measured Desiccation Efficiencies with Different Parameters of Mouthpiece Construction

length (mm)	diameter (mm)	particle size (mm)	porosity	simulated efficiency (%)	measured efficiency (%)	difference in efficiency (%)
12	22	1.15	0.425	44.1	43.6	0.5
25	22	1.15	0.425	68.8	66.49	2.31
49	22	1.15	0.425	89.3	81.54	7.76
12	22	0.65	0.365	58.5	61	2.5
15	22	0.65	0.365	69.6	68.4	1.2

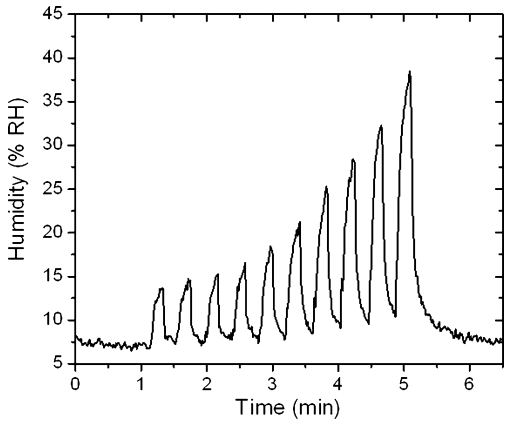

Figure 8. Humidity output of the mouthpiece (15 mm diameter, 30 mm length, 5 g of calcium chloride, 1.15 mm particle diameter, porosity of 0.425) for ten successive breathings. The baseline was obtained with dry air purging.

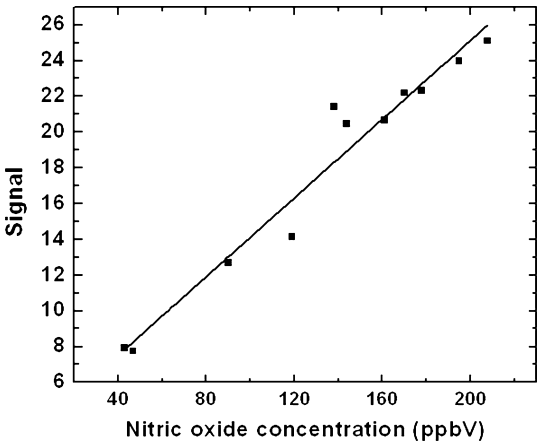

Figure 10. Analysis of nitric oxide levels in a breath sample using a colorimetric optical sensor integrated with the desiccation mouthpiece for online sample conditioning. A linear response is obtained toward nitric oxide.

Table 2 shows a comparison of simulated and measured desiccation efficiencies for different mouthpiece geometries, packing, and particle sizes. Deviations in the results increase at high desiccation efficiencies. With increasing desiccation, the experimental efficiency is lower than the predicted efficiency from the model. This could be attributed to the exothermic nature of the desiccation process which starts to affect the efficiency for high humidity capture. Due to higher surface temperature, the actual efficiency of capture is lower as observed in the experimental results.

Figure 8 shows humidity output of the mouthpiece over ten successive breathings measured by SIFT-MS. Each exhalation was followed by purging with dry air sample. It can be observed that the output was much drier initially and the efficiency of the mouthpiece decreased with successive breathing cycles due to exhaustion and heating although the average humidity remained within the desired noncondensing levels.

Integration with Portable Breath Sensors. A desiccant mouthpiece with an average efficiency of 70% (30 s sampling at 6.67 mL·min^{-1}) was used to sample breath in a colorimetric optical sensor developed in our lab. Figure 9A shows the response of the sensor to breath sampling without the mouthpiece. A jump in the intensity of signal can be observed in the sensing photodiode due to humidity condensation on the substrate affecting the transmittance.[37] Also, the reference photodiode shows random fluctuations in the signal. Response of the same sensor after integration of the mouthpiece is shown in Figure 9B. A linear decrease in intensity due to color development is observed without any spike due to humidity on the sensing photodiode. The reference photodiode also shows a

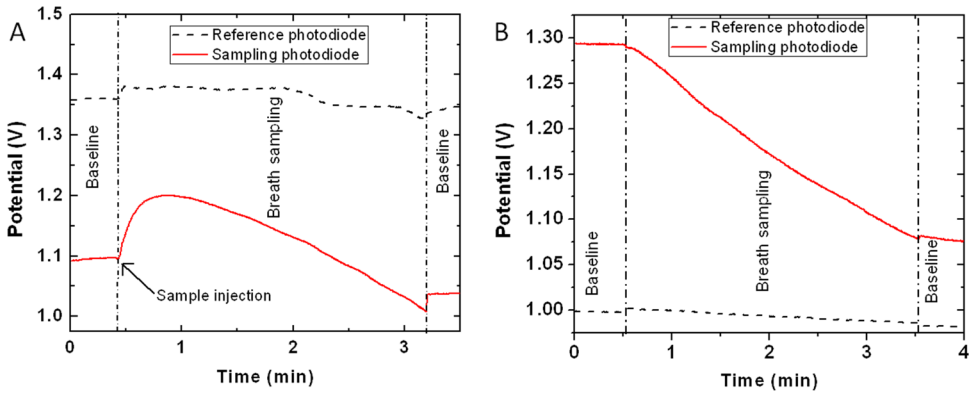

Figure 9. Optical response from photodiodes used for detection of color change (sampling) and correction (reference) in intensity during breath test (A) without the use of a desiccant mouthpiece and (B) after integration of the desiccant mouthpiece.

dx.doi.org/10.1021/ac301542j | Anal. Chem. 2012, 84, 7172−7178

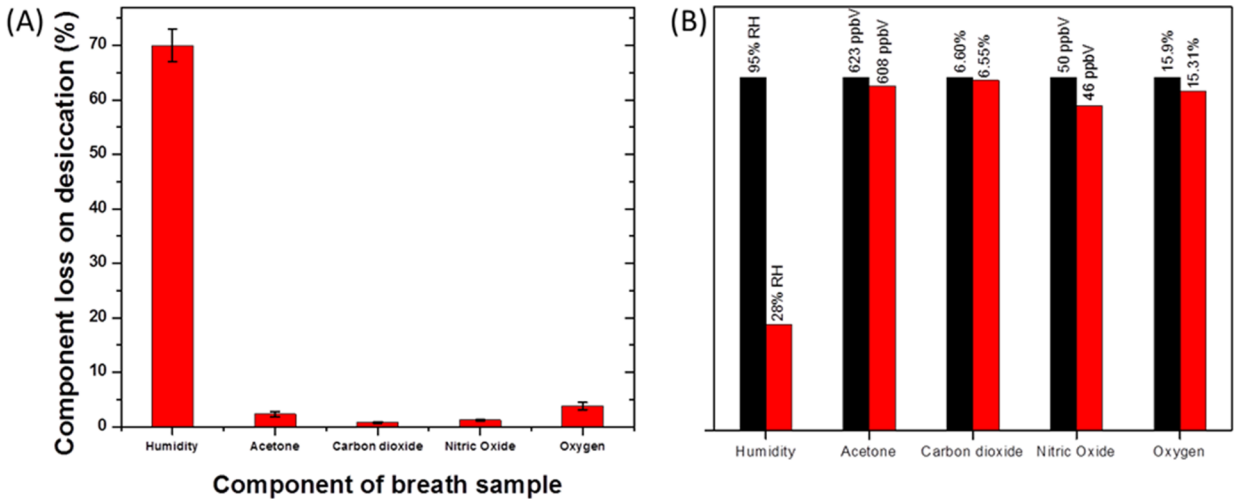

Figure 11. (A) Selective removal of humidity by the desiccant mouthpiece over other components of interest. (B) Absolute value of concentrations for different compounds tested before and after passing through the mouthpiece.

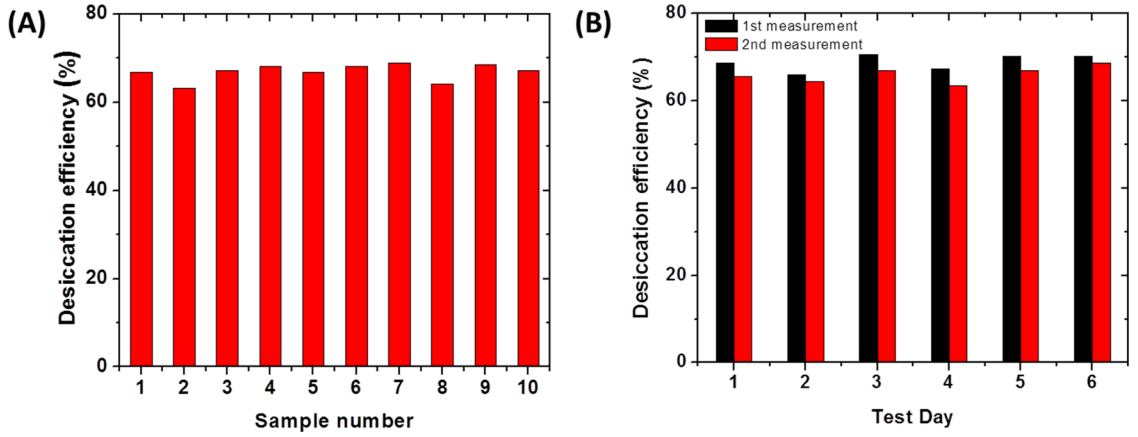

Figure 12. (A) Efficiency and reusability of one mouthpiece with a 10 min gap between successive tests. Mean desiccation efficiency (%) = 67.3% and variation from the mean is 5.6% (B) Reusability of one mouthpiece over a week measured two times each day and stored in ambient lab conditions in a zip-lock bag. Mean desiccation efficiency (%) = 67.17% and variation from the mean is 3.4%.

stable signal, and fluctuations due to humidity are not observed. After integration of the mouthpiece, real breath samples could be analyzed for nitric oxide using the portable device as shown in Figure 10.

Selectivity of the Desiccation Material. The desiccation mouthpiece made of calcium chloride was tested for capture of some other gases including acetone, carbon dioxide, nitric oxide, and oxygen for which the mouthpiece showed a capture efficiency of less than 5% for a 70% removal of humidity (Figure 11). These results show that the desiccant material can be used for analysis of these gases in conditioned breath by suitable sensors. However, there are some gases which can be captured by calcium chloride along with humidity. Ammonia is known to form a complex with calcium chloride.[38] 10 ppmV input ammonia reduced to 0.8 ppmV output resulting in 92% ammonia removal efficiency of the calcium chloride mouthpiece under similar configuration.

Reusability of the Mouthpiece. Reusability of the mouthpiece was tested for conditioning of real samples. Figure 12A shows the efficiency of desiccation with variation of 5.6% at a mean efficiency level of 67.3% using a single mouthpiece (23 cm length, 22 mm diameter, particle size of 1.15 mm, porosity of 0.425) for collection of ten samples with gap of 10 min between successive tests. Each sample was collected at a flow rate of 6.7 L/min to fill a 4-L Tedlar bag. A gap of 10 min was given between each collection which was necessary to avoid efficiency loss due to overheating of the tube. The desiccation tube was also used for routine testing over a week. A single mouthpiece was used for sample collection, two times a day separated by 6 to 8 h for six consecutive days. Figure 12B shows the desiccation efficiency of each test. The mean efficiency for the six day test was 67.17% with a variation of 3.4%. The mouthpiece was stored in a regular zip-lock bag after each test. The storage was necessary because calcium chloride being hygroscopic adsorbs water continuously from the atmosphere. The zip-lock bag insulated the mouthpiece from the environment and allowed excessive humidity capture to be avoided, which slowed the exhaustion of the mouthpiece.

■ CONCLUSIONS

A miniaturized mouthpiece was developed to efficiently remove humidity and condition real breath samples in real time without affecting target analyte concentrations. The mouthpiece consists of packed desiccant particles in a tube. Numerical simulation of the desiccation process was carried out by taking into account various processes, including diffusion, mass

dx.doi.org/10.1021/ac301542j | Anal. Chem. 2012, 84, 7172−7178

transport, and water absorption, described by differential equations with appropriate boundary conditions. The performance the mouthpiece in terms of humidity control and backpressure minimization depends on the size and packing density of the particles, geometry of the tube, and flow rate. On the basis of the simulation, mouthpieces with different configurations were built and tested, and the experimental results validated the simulation findings. The findings provide guidance for those who wish to design efficient sample conditioning systems for practical chemical sensors, particularly breath analyzers. The mouthpiece was integrated into a hand-held sensor for exhaled nitric oxide detection, and the results are in excellent agreement with gold standard methods. The miniaturized mouthpiece has great applicability for the new generation of portable breath analyzers, which require easy, efficient, and reproducible removal of high humidity for seamless device functioning.

AUTHOR INFORMATION

Corresponding Author

*E-mail: nongjian.tao@asu.edu.

Notes

The authors declare no competing financial interest.

ACKNOWLEDGMENTS

This work has been supported by NIBIB/NIH (#1R21EB014219-01) through the Technologies for Health Independent Living Program (Director: Dr. Brenda Korte). We are thankful to collaborators Rui Wang and Di Zhao from Center for Bioelectronics and Biosensors, Biodesign Institute, who have contributed to this work with suggestions and ideas about different modeling approaches and applications of use.

REFERENCES

(1) Pauling, L.; et al. *Proc. Natl. Acad. Sci.* **1971**, *68* (10), 2374.
(2) Sanchez, J. M.; Sacks, R. D. *Anal. Chem.* **2003**, *75* (10), 2231–2236.
(3) Španel, P.; Smith, D. *Curr. Opin. Clin. Nutr. Metab. Care* **2011**, *14* (5), 455.
(4) Smith, A. D.; et al. *N. Engl. J. Med.* **2005**, *352* (21), 2163–2173.
(5) Levitt, M. D.; Donaldson, R. *J. Lab. Clin. Med.* **1970**, *75* (6), 937.
(6) Rowland, M.; et al. *J. Pediatr.* **1997**, *131* (6), 815–820.
(7) Gisbert, J.; Pajares, J. *Aliment. Pharmacol. Ther.* **2004**, *20* (10), 1001–1017.
(8) Cao, W.; Duan, Y. *Clin. Chem.* **2006**, *52* (5), 800.
(9) Beauchamp, J. *J. Breath Res.* **2011**, *5*, 037103.
(10) Ochiai, N.; et al. *J. Chromatogr., B: Biomed. Sci. Appl.* **2001**, *762* (1), 67–75.
(11) Grote, C.; Pawliszyn, J. *Anal. Chem.* **1997**, *69* (4), 587–596.
(12) Robinson, J. K.; Bollinger, M. J.; Birks, J. W. *Anal. Chem.* **1999**, *71* (22), 5131–5136.
(13) Konvalina, G.; Haick, H. *ACS Appl. Mater. Interfaces* **2012**, *4* (1), 317–325.
(14) Burns, W. F.; et al. *J. Chromatogr., A* **1983**, *269* (0), 1–9.
(15) Foulger, B. E.; Simmonds, P. G. *Anal. Chem.* **1979**, *51* (7), 1089–1090.
(16) Leckrone, K. J.; Hayes, J. M. *Anal. Chem.* **1997**, *69* (5), 911–918.
(17) Španěl, P.; Smith, D. *Rapid Commun. Mass Spectrom.* **2001**, *15* (8), 563–569.
(18) Boshier, P. R.; et al. *Analyst* **2011**, *136* (16), 3233–3237.
(19) King, J.; et al. *J. Math. Biol.* **2011**, *63* (5), 959–999.
(20) King, J.; et al. *J. Theor. Biol.* **2010**, *267* (4), 626–637.
(21) King, J.; et al. *J. Breath Res.* **2012**, *6*, 016005.
(22) Diskin, A. M.; Španěl, P.; Smith, D. *Physiol. Meas.* **2003**, *24*, 107.
(23) King, J.; et al. *Physiol. Meas.* **2010**, *31*, 1169.
(24) King, J.; et al. *Physiol. Meas.* **2012**, *33*, 413.
(25) American Thoracic Society. *Am. J. Respir. Crit. Care Med.* **2005**, *171*, 912–930.
(26) Prabhakar, A.; Iglesias, R. A.; Wang, R.; Tsow, F.; Forzani, E. S.; Tao, N. *Anal. Chem.* **2010**, *82* (23), 9938–9940.
(27) Childs, E.; Collis-George, N. *Proc. R. Soc. London. Ser. A.: Math. Phys. Sci.* **1950**, *201* (1066), 392–405.
(28) Bear, J. *Dynamics of fluids in porous media*; Dover publications: Mineola, NY, 1988.
(29) Tsilingiris, P. *Energy Convers. Manage.* **2008**, *49* (5), 1098–1110.
(30) Zhang, X.; Qiu, L. *Energy Convers. Manage.* **2007**, *48* (1), 320–326.
(31) Glueckauf, E.; Coates, J. *J. Chem. Soc.* **1947**, 1315–1321.
(32) Sircar, S.; Hufton, J. *Adsorption* **2000**, *6* (2), 137–147.
(33) Joly, A.; Volpert, V.; Perrard, A. Dynamic Adsorption with FEMLAB, Modeling breakthrough curves of gaseous pollutants through activated carbon beds. *Proceedings of the Comsol Multiphysics Conference*, Comsol France, Paris, 2005; pp. 277–282.
(34) Park, I.; Knaebel, K. S. *AIChE J.* **1992**, *38* (5), 660–670.
(35) Kamiuto, K.; Ermalina; Ihara, K. *Appl. Energy* **2001**, *69* (4), 285–292.
(36) Mămăligă, I.; Baciu, C.; Petrescu, S. *Environ. Eng. Manage. J. (EEMJ)* **2009**, *8* (2), 253–257.
(37) Ellerbee, A. K.; et al. *Anal. Chem.* **2009**, *81* (20), 8447–8452.
(38) Popov, A. I.; Wendlandt, W. W. *J. Am. Chem. Soc.* **1955**, *77* (4), 857–859.